



Total oxidation of trichloroethylene over mayenite ($\text{Ca}_{12}\text{Al}_{14}\text{O}_{33}$) catalyst



Raffaele Cucciniello^{a,1}, Adriano Intiso^{a,1}, Stefano Castiglione^a, Alessandra Genga^b, Antonio Proto^a, Federico Rossi^{a,*}

^a Dipartimento di Chimica e Biologia, Università di Salerno, via Giovanni Paolo II, 132, 84084, Fisciano, Salerno, Italy

^b Dipartimento di Scienze Tecnologiche, Biologiche ed Ambientali, Università del Salento, 73100, Lecce, Lecce, Italy

ARTICLE INFO

Article history:

Received 31 August 2016

Received in revised form

14 November 2016

Accepted 16 November 2016

Available online 17 November 2016

Keywords:

Mayenite

Trichloroethylene

Catalytic oxidation

Chlorinated VOCs

ABSTRACT

The catalytic oxidation of gaseous trichloroethylene (TCE), mediated by a cost effective mayenite support, was studied in a fixed bed reactor. Mayenite was synthesized by using hydrothermal method and characterized before and after catalytic oxidation experiments by using XRD, N_2 -sorption (BET), SEM-EDX, TEM and FTIR; the reaction products were analyzed by means of GC-MS, IC and a IR-based CO_2 probe. The results showed that mayenite promoted the total oxidation of TCE in the temperature range 300–500 °C, where TCE was quantitatively converted in CO_2 and chlorine. The mayenite catalyst showed high recyclability and could be used for several reaction cycles without any loss of activity and selectivity. Owing to its characteristics, mayenite was found to be a promising catalyst for the TCE total conversion and remediation.

© 2016 Elsevier B.V. All rights reserved.

1. Introduction

Trichloroethylene (TCE) is a common chlorinated volatile organic compound (CVOC), generally employed as degreasing agent and in dry-cleaning applications [1]. Nowadays, TCE has become a dangerous pollutant, being toxic, chemically stable and carcinogenic for humans [2]. TCE shows a low solubility in water, high density ($>1\text{ g cm}^{-3}$) and high affinity for organic compounds [3]. From an environmental point of view, the use of TCE as cleaning product has been prohibited since at least twenty years [4], however several pollution cases have been recorded [5]; TCE is considered one of the components of the photochemical smog [6] and it is one of the major contaminants of the aquifers [7], especially because of its density that causes the stratification at the bottom of groundwater. In the last years, several strategies have been developed for the removal of TCE including pump and treat, surface enhanced dissolution, adsorption processes, air stripping and phytoremediation [1,8–10]. Furthermore, after the TCE removal from the environment several technologies were used for its complete destruction and thermal and catalytic routes were the

most investigated [11]. Thermal incineration was, by far, the most used technology, but it showed high costs related to the operative temperature, often higher than 700 °C, and limitations connected to the chlorinated by-products formation. Therefore, the catalytic oxidation of TCE represented an interesting alternative that permits to operate at lower temperatures (250–550 °C) with a drastic reduction of energetic costs. Furthermore, a specific catalyst design can favour the reaction selectivity in the direction of the desired products, limiting the by-product formation. Many recent works reported the preparation of catalysts able to oxidize and quantitatively convert trichloroethylene [12–14]. About the proposed catalysts, metal oxides and supported noble metals were generally preferred. However, they also have some limitations due to the formation of chlorinated by-products, such as perchloroethylene (PCE) [15]. Blanch-Raga et al. [16] prepared and used hydrotalcite-like compounds to host metal catalysts, such as $\text{Mg}(\text{Fe}/\text{Al})$, $\text{Ni}(\text{Fe}/\text{Al})$ and $\text{Co}(\text{Fe}/\text{Al})$, showing good performances for the TCE oxidation, mainly due to the presence of O_2^- and O_2^{2-} sites that enhance the catalytic productivity. At the same time, the authors observed the formation of several by-products (HCl , PCE and Cl_2). Zeolites based catalysts were also tested, and they showed a good productivity but a rather low recyclability, the latter due to coke deposition and acidic sites deactivation promoted by the chlorine [17]. In this context, many efforts are directed towards the research of new catalysts able to oxidize TCE with high productivity, selectivity and recyclability. The use of noble or transition metals free catalysts has

* Corresponding author at: Università degli Studi di Salerno, via Giovanni Paolo II, 132, 84084 Fisciano, Salerno, Italy.

E-mail address: frossi@unisa.it (F. Rossi).

¹ These authors contributed equally.

to be preferred to avoid the metals depletion and the high costs for their recovery at the end of the material life-cycle [18].

Mayenite ($\text{Ca}_{12}\text{Al}_{14}\text{O}_{33}$) is a mesoporous calcium aluminium oxide, labelled C12A7 ($12\text{CaO} \cdot 7\text{Al}_2\text{O}_3$), with a characteristic crystalline structure. In contrast to aluminosilicate zeolites, the framework of mayenite is composed of interconnected cages with a positively electric charge per unit cell that includes two molecules, $[\text{Ca}_{24}\text{Al}_{28}\text{O}_{64}]^{4+}$, and the remaining two oxide ions O^{2-} , often labelled “free oxygen”, were trapped in the cages defined by the framework [19]. In the last years, the formation and desorption mechanisms of oxygen species in mayenite have been investigated by using electronic spin-resonance (ESR) and raman spectroscopy (RS) showing high concentrations ($\approx 10^{20} \text{ cm}^{-3}$) of reactive oxygen species [20,21]. Mayenite derivatives obtained by substituting the free oxygen ions with other anions (Cl^- , H^- , O^- , OH^- , NH_2^- , e^- , etc.) have prepared and used in several research fields [22–24]. The ability of storing O^{2-} ions in the cages is a prominent property of mayenite and it was exploited in catalysis because oxygen ions can migrate between the surface and the bulk at temperature higher than 400°C , showing a unique ionic conductivity [25]. For example, Ruszak and coworkers exploited the oxidation ability of mayenite for the selective decomposition of N_2O [26]. Also, Li et al. used mayenite as active support for Ni catalyst for the biomass tar steam reforming, thus avoiding the undesirable coke formation, typical of the zeolites [27].

In this work, we report on the use of undoped mayenite as catalyst for the total oxidation of gaseous TCE. The catalyst was prepared by using a hydrothermal method and TCE oxidation was carried out in a stainless steel fixed bed reactor. The reaction products were analyzed by means of GC–MS, IC and a IR-based CO_2 probe; good results were obtained in terms of activity and selectivity and a plausible stoichiometry was finally proposed.

2. Experimental

2.1. Catalyst preparation

Mayenite based catalyst was prepared by following the hydrothermal method proposed by Li et al. [28], as follows: a stoichiometric mixture of $\text{Ca}(\text{OH})_2$ and $\text{Al}(\text{OH})_3$, 41.5 and 50.7 g respectively, was added to 1 L of distilled water. The mixture was grounded under magnetic stirring for 4 h at room temperature, afterwards, was placed in stainless steel autoclave at 150°C for 5 h. The obtained solid was filtrated and dried at 120°C overnight, crushed into fine powder and finally placed into a furnace at 1000°C in air for 4 h.

2.2. Mayenite catalyst characterization

X-ray diffraction patterns were obtained on a Bruker D8 Advance automatic diffractometer operating with a nickel-filtered $\text{CuK}\alpha$ radiation. Data were recorded in the 2θ range of $4\text{--}80^\circ$ with the resolution of 0.02° . The BET surface area of the catalyst was determined using a Nova Quantachrome 4200e instrument using nitrogen as the probe molecule at liquid nitrogen temperature (-196°C). Before the adsorption measurement, mayenite sample was degassed at 200°C under vacuum for 12 h. The surface area values were determined by using 11-point BET analysis.

Particle sizing experiments were carried out by means of laser diffractometer, using an Mastersizer 2000 instrument (Malvern Instrument Ltd) operating at 25°C . The morphological and elemental analyses were performed by a scanning electron microscope (SEM, Tescan Vega LMU) equipped with a X-Ray energy dispersive microanalysis of elements having an atomic number >4 , with a resolution of $\text{MnK}\alpha$ less than 123 eV (100,000 cps) (EDX, Bruker Quantax 800). Mayenite samples were placed on stubs covered by carbon disk. SEM images were obtained by secondary electrons (SE) with an accelerating voltage of 20,00 kV. The EDX spectra were obtained with an accelerating voltage of 20,00 kV and with a WD of 15,0 mm. X-Ray intensities were converted in wt% elements by a standardless ZAF quantification. TEM images were obtained using a TECNAI 20 G2: FEI COMPANY (CRYO-TEM-TOMOGRAPHY, Eindhoven) with a camera Eagle 2HS. The images were acquired at 200 kV; camera exposure time: 1 s; size 2048×2048 . FTIR spectroscopic measurements were carried out using a Vertex 70 FTIR spectrometer from Bruker equipped with deuterated triglycine sulfate (DTGS) detector and a Ge/KBr beam splitter. Infrared spectra were acquired in the range of $4000\text{--}400 \text{ cm}^{-1}$ at a resolution of 2.0 cm^{-1} . The analyses were carried out on a pressed mixture prepared by using about 3 mg of sample in 100 mg of dried KBr.

2.3. Apparatus and catalytic reactions

Experiments were carried out at atmospheric pressure in a stainless-steel fixed bed reactor (150 mm long, 22 mm o.d, 18 mm i.d) schematically shown in Fig. 1. The catalytic bed (0.8 g of mayenite) was placed into the reactor between two quartz fiberglass layers. The reactor was placed in an electrically-heated furnace, and the temperature was measured by a K-thermocouple. Catalytic oxidation reactions were carried out at different temperature, between 25°C and 500°C for 0.09 h. Mayenite was conditioned at the operative temperature with air for 30 min prior the TCE injections. The gaseous mixture, composed by trichloroethylene (1700 ppm) and wet air ($\text{RH} = 60\%$), was introduced into the reactor at 110 mL/min

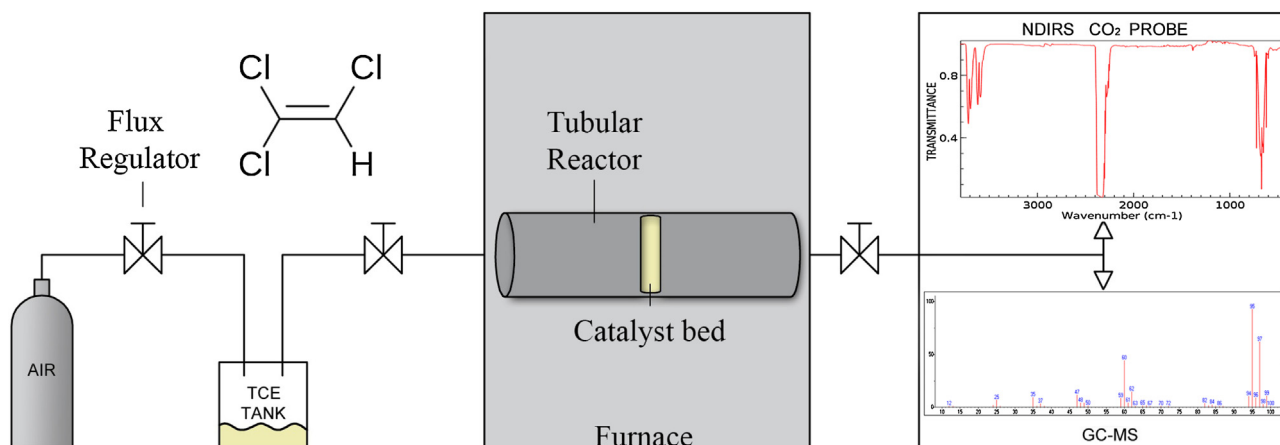


Fig. 1. Sketch of the experimental setup.

(Gas Hourly Space Velocity, GHSV = 6000 h⁻¹). The gaseous mixture was prepared by sparging with air a vessel containing 1 μ L of pure TCE. Blank experiments were made in the same conditions without the presence of the catalyst for all the investigated temperatures.

2.4. Gas analysis and products characterization

Gaseous reaction products were collected in a Tedlar sampling bag (SKC, Inc., USA) before analyses. TCE and VOCs concentrations were determined by gas chromatography by using a GC–MS (Agilent 7890A) equipped with a DB 17-MS column (30 m \times 0.25 mm 250 μ m). A GC oven was run isothermally at 100 °C for 10 min. Helium was used as carrier gas with a flow rate of 0.5 mL/min and 1.0 mL of sample was analyzed in a split-less injection mode. NDIRS on line probe (Q-Track Plus IAQ Monitor, TSI) was coupled to the reactor to monitor the concentration of CO₂ and CO resulting from TCE oxidation and the relative humidity (RH%) [29]. Molecular chlorine, Cl₂ (m/z = 71), was determined by SIM mode GC–MS analysis [30], using the same operative conditions described for VOCs analysis. Moreover, the production of Cl₂ was also checked by means of iodometric titration, by bubbling the effluent stream through a 0.06 M solution of KI and 0.1 M of H₂SO₄ using soluble starch as indicator.

Cl⁻ ions were determined by bubbling the effluent into a 2.6/0.76 mM solution of NaHCO₃/Na₂CO₃ and analyzing the resulting chloride amount through ion chromatography (IC) using a Dionex DX 120 (Dionex, Sunnyvale, CA, USA) equipped with an Ion Pac AS14 column (4 mm \times 250 mm). Moreover 0.5 g of mayenite were extracted with 3 mL of 2.6/0.76 mM solution of NaHCO₃/Na₂CO₃ and analyzed by means of IC with the same experimental conditions used for the gas.

The conversion yield of TCE was defined as the ratio between the reacted TCE over the total TCE delivered into the reactor and it can be calculated by means of equation (1.1)

$$\text{TCE conversion [\%]} = \frac{m_{\text{TCE}}^i - m_{\text{TCE}}^o}{m_{\text{TCE}}^i} \times 100 \quad (1.1)$$

where m_{TCE}^i are the moles of TCE delivered into the reactor and m_{TCE}^o are the number of moles measured at the reactor outlet.

3. Results and discussion

The catalytic material, mayenite, was prepared, according to the *hydrothermal* method, by mixing and calcinating a mixture of calcium and aluminium hydroxides. The crystalline structure of the mayenite was investigated by means of x-ray diffractometry and the mayenite typical diffraction spectrum is reported in Fig. 2. Catalyst structure was indexed within *I*-43d group. The mayenite XRD pattern presents the characteristic peaks of mayenite around 2θ = 18.1°, 30°, 33.4°, 36.7°, 41.2°, 46.7°, 55.2° and 57.4°. Ca₃Al₂O₆ (●) and CaAl₂O₄ (◆) were also detected in trace as usual impurities formed during the mayenite preparation processes [25].

Synthesized mayenite showed a BET surface area of 4.5 m²/g, in line with data reported in the literature [26] for this type of materials and a particle sizing of 70 μ m.

To assess the efficiency of mayenite in degrading trichloroethylene, we tested the catalytic material by using the reactor reported in Fig. 1 at different temperatures, ranging in the interval 25–500 °C. In particular, for all the temperatures investigated the concentration of TCE in the flowing air stream (1700 ppm) and the GHSV (6000 h⁻¹) were kept constant. The presence of TCE in the out-flowing stream at the reactor exit was monitored by means of a GC–MS apparatus. Fig. 3 shows the degradation yield expressed as the percentage of TCE converted during the catalytic reaction and calculated by means of Eq. 1. For low temperatures (<300 °C)

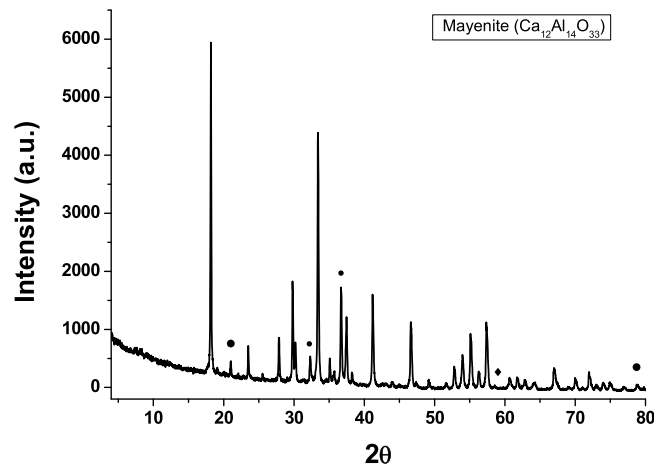


Fig. 2. XRD pattern of mayenite (Ca₁₂Al₁₄O₃₃).

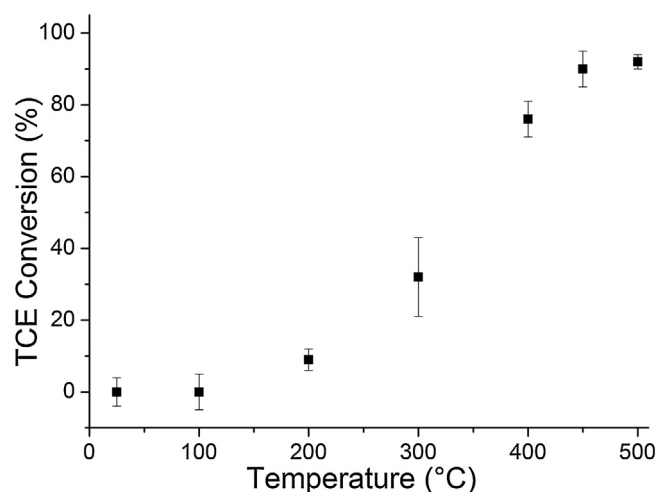


Fig. 3. TCE conversion rate for the oxidation reaction over mayenite catalyst at different temperatures.

Table 1

TCE conversion using mayenite catalyst.

Temperature (°C)	TCE Conversion (%)
25	N.N.
100	N.N.
200	9 ± 3
300	32 ± 11
400	76 ± 5
450	90 ± 5
500	92 ± 2

we could not observe a significant degradation of the chlorinated compound and the concentration of TCE at the reactor outlet was found the same as at the reactor inlet. The catalytic oxidation of trichloroethylene started at 300 °C where 32% of the delivered TCE was converted. The conversion yield was found to increase drastically with the temperature, as reported in Fig. 3 and Table 1, and it passed from 26% to 76% and 90% for a temperature of 400 °C and 450 °C, respectively. As mentioned in the introduction, the free oxygen present in the mayenite framework was the active species responsible for the TCE degradation. This is consistent with the temperature dependence of the conversion yield; in fact, as reported in previous works [31], mayenite, at higher temperatures, interacts with the atmospheric O₂ to form reactive oxygen species (O²⁻, O⁻, O₂⁻) that, in turn, can react and oxidize TCE to CO₂.

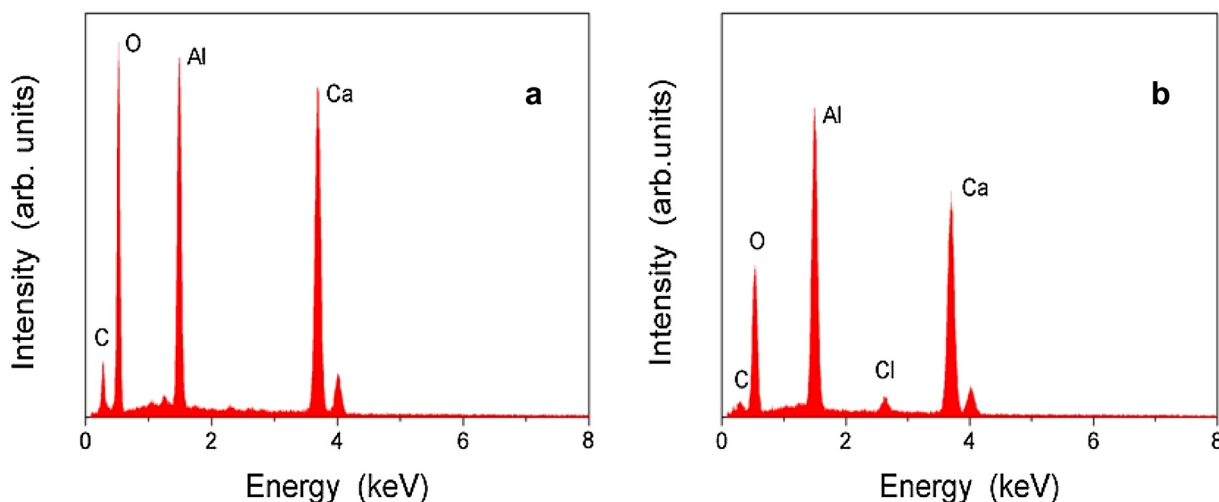


Fig. 4. EDX spectra of mayenite (a) before and (b) after the oxidation reaction.

Blank experiments, performed without using mayenite at any investigated temperatures, have no shown significant results in terms of TCE conversion.

To understand the reaction mechanism and to characterize the reaction products, GC–MS analyses were performed in full-spectrum mode to detect the presence of other organic compounds. Moreover a NDIRS technique was used to monitor the presence of CO_x species. Both the chromatographic and the IR analyses showed that the only carbon-containing product was CO_2 , and no other organic compounds could be detected with both the techniques. It is important to underline that no CO was detected at any investigated temperature showing a good catalyst selectivity.

The analyses of chlorinated derivatives of TCE were performed by means of ionic chromatography and iodometric titration. In particular, we were interested in finding chlorine-derivatives in the form of molecular chlorine, Cl_2 , chloride ions, Cl^- , or chlorine-oxo species, ClO_x , as generally resulting from the TCE decomposition [13,16]. Iodometric titration did not reveal the presence of Cl_2 and this result was also confirmed by GC–MS analysis in SIM mode, centered on the mass $m/z = 70 \pm 1$. To find Cl^- and ClO_x both the gases at the exit of the reactor and the catalytic material were analyzed. Gases were bubbled in an aqueous solution of $\text{NaHCO}_3/\text{Na}_2\text{CO}_3$ and 20 μL of the solution were injected in an ionic chromatograph equipped with a negatively charged column for anion detection. The same procedure was applied for the analysis of the mayenite, which was extracted with the carbonate buffer. IC revealed that Cl^- ions were present only on the catalytic material and no other chlorinated species were detected in the gases or in the mayenite. This result is consistent with the fact that mayenite tends to adsorb Cl^- to form chloromayenite (Brearleyite, $\text{Ca}_{12}\text{Al}_{14}\text{O}_{32}\text{Cl}_2$) due to the substitution of free oxygen molecules with chlorides [32].

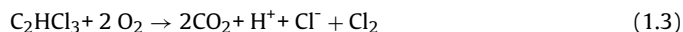
These results were also confirmed by SEM–EDX analysis. EDX analysis of the material shows that synthesized mayenite is characterized by the presence of Ca, Al and O (Fig. 4a) in atomic ratios of $1:0.96 \pm 0.17:3.1 \pm 0.3$, in line with the theoretical value for pure mayenite. After the oxidation reaction, Ca, Al and O are still detected (Fig. 4b) but the signal of Cl can be pointed out. EDX analysis shows that Cl is uniformly distributed on mayenite sample ($3.0 \pm 1.1\%$ wt) and that there is a decrease of oxygen content. Ca, Al, O and Cl show atomic ratios of $1:0.95 \pm 0.16:2.9 \pm 0.3:0.10 \pm 0.05$, which are consistent with the formation of chloromayenite. The signal of C has not been taken into account in each spectra, because the samples have been placed on carbon disk and there is not statistically dif-

ference between C signal from the mayenite samples and from the substrate.

Qualitative analyses of the *post-reaction* gases and of the catalytic material revealed that the only products of the decomposition of TCE are CO_2 and Cl^- ; The general balanced reaction should have the form:



at this stage it is difficult to define a complete reaction mechanism; in fact Cl^- ions could also be the result of the interaction of Cl_2 , formed in a first stage of the oxidation, with the air moisture and the catalytic material. In this respect, it is known that mayenite can interact with chloride salts to form stable chloro-derivatives [33]. A plausible step in the reaction scheme can be



To support our hypothesis, at 500°C we quantified the amount of CO_2 and Cl^- detected in the gases and on the mayenite catalyst, respectively, after the treatment of 1.5 mg (~ 0.01 mmol) of TCE. Carbon dioxide measurements were performed by means of a NDIRS probe and 1.0 mg, corresponding to ~ 0.022 mmol, of CO_2 were detected. The mass balance resulted, therefore, in agreement with the theoretical stoichiometry (1:2) of reaction (1.2). The same result was observed for Cl^- ions, measured by means of ionic chromatography after extraction of the catalyst with a carbonate buffer solution; in this case 1.1 mg of Cl^- (~ 0.03 mmol) were detected, corresponding to a stoichiometric factor 1:3 as in the reaction (1.2).

Results are in agreement with those reported by Aranzabal in a recent review, where the presence of water enhances the reaction selectivity towards HCl and CO_2 [34].

Catalyst recyclability was tested at 500°C where the oxidation of TCE was found to be quantitative. After each experiment we restored the catalytic properties of the mayenite by treatment at 500°C in wet air for 10 min, so that reaction products (e.g. chlorine) could be replaced by free oxygen ions. As clearly shown in Fig. 5, the catalyst is stable at this temperature without any significant loss in activity and selectivity also after 3 h of reaction. Afterwards, we observed a partial deactivation of the catalyst due to the displacing of the active oxygen species by chloride and the conversion decreases from 95% to 84% after 12 h of reaction.

XRD patterns of mayenite, before and after catalytic oxidation reaction, are reported in Fig. 6. Results show only a crystalline structure change of the mayenite catalyst due to the reaction conditions (500°C). More detailed information are reported in the supporting material.

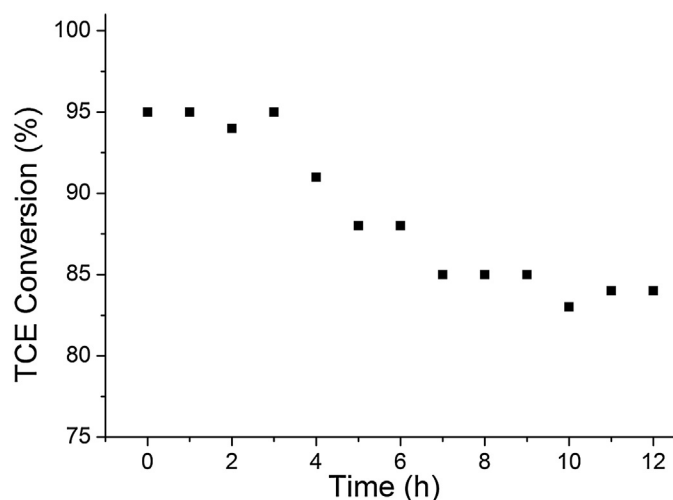


Fig. 5. Stability of the mayenite catalyst (reaction conditions: $T_{95} = 500^{\circ}\text{C}$, $[\text{TCE}]_{\text{inlet}} = 1700 \text{ ppm}$, $\text{GHSV} = 6000 \text{ h}^{-1}$, 0.8 g of catalyst).

In Fig. 7a and b SEM images of mayenite before and after the oxidation reaction are reported, respectively.

Any significant morphological changes are detected before and after the oxidation reaction and mayenite is characterized by significant porosity which still remain (Fig. 7b). In fact, the presence of sheets and two types of pores can be pointed out: large macropores on the μm scale and mesopores on the nm scale. FTIR and TEM analyses also confirm that no change in the mayenite structure and morphology has been detected after several catalytic cycles (see supporting materials).

In terms of TCE conversion yield, mayenite (90% at 450°C) showed better performances than metal undoped zeolites (<10% at 400°C) and in line with the metal-loaded zeolites (90–95% at 350°C) [16]. Moreover, respect to previous catalytic systems, mayenite presented several distinctive advantages, namely *i*) a total conversion of TCE in less harmful Cl^{-} and CO_2 , *ii*) the presence of free O^{2-} ions made unnecessary the use of noble and heavy metals, thus reducing the costs and the environmental impact at the end of the material life-cycle and *iii*) inexpensive precursors for the material synthesis, such as calcium and aluminium hydroxides.

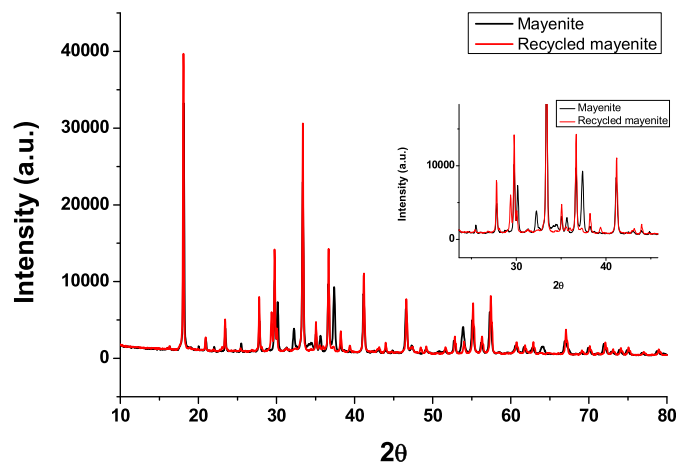


Fig. 6. XRD patterns of mayenite before (black line) and after (red line) catalytic oxidation reaction. The inset shows a detail of the range $20 < 2\theta < 50$. (For interpretation of the references to colour in this figure legend, the reader is referred to the web version of this article.)

4. Conclusions

In this work, we studied for first time the catalytic activity for the TCE oxidation of the mayenite catalyst, prepared by hydrothermal synthesis. The results showed that mayenite was an active catalyst for the TCE oxidation. TCE was totally converted in CO_2 and the released chlorine was incorporated in the mayenite structure. The high performances of the catalyst could be connected to its oxidative properties due to the presence of O^{2-} and O_2^{2-} anions sites that favour the total oxidation of TCE and avoid the formation of coke. Catalyst shows high recyclability and thermal stability being reused several times without losses in activity and selectivity operating at temperatures lower than those reported for metal supported based catalysts. In this way this material can be considered an effective active catalyst for the TCE oxidation and it enriches the pool of possible catalysts for this application. At this stage it is difficult to describe the complete reaction mechanism and further studies are planned to assess the role of the air moisture in promoting the TCE decomposition. However, our results encourage further studies for in-field applications.

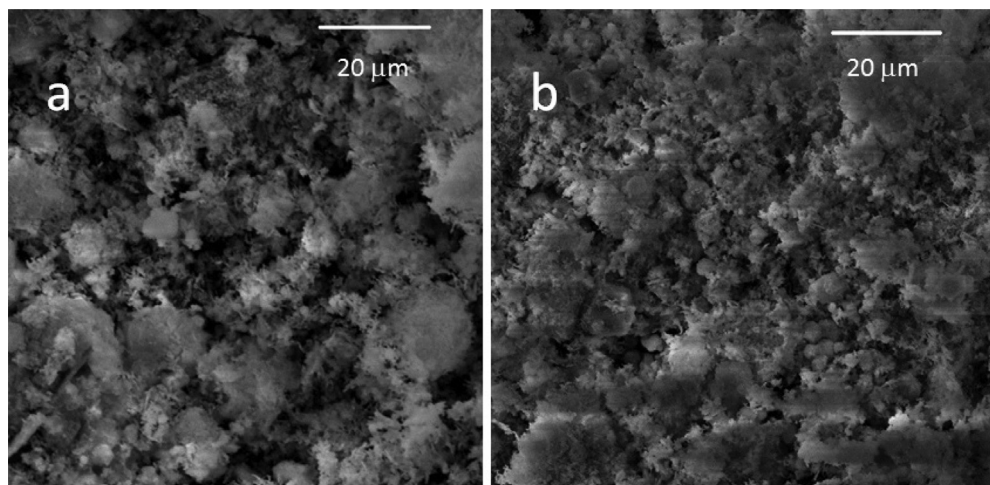


Fig. 7. SEM images of mayenite (a) before oxidation reaction and (b) after oxidation reaction.

Acknowledgements

This work was supported by the grants ORSA158121 and ORSA149477 funded by the University of Salerno. Authors dedicate this article to the memory of Mr. Antonio Mormile, for its helpful discussions and technical assistance during the last twenty years of collaboration. Authors are also in debt with Dr. Emanuele Moccia, Dr. Maurizio Celentano and Mr. Michele Napoli for technical assistance.

Appendix A. Supplementary data

Supplementary data associated with this article can be found, in the online version, at <http://dx.doi.org/10.1016/j.apcatb.2016.11.035>.

References

- [1] H.L. Greene, D.S. Prakash, K.V. Athota, *Appl. Catal. B: Environ.* 7 (1996) 213–224.
- [2] J. Caldwell, A. Blair, R.J. Bull, B. Charbotel, Trichloroethylene Tetrachloroethylene and some other chlorinated agents IARC Monographs on the Evaluation of Carcinogenic Risks to Humans, vol. 106, IARC (International Agency for Research on Cancer), 2014, pp. 1–514.
- [3] F. Rossi, R. Cucciniello, A. Intiso, A. Proto, O. Motta, N. Marchettini, *AIChE J.* 61 (2015) 3511–3515.
- [4] R.E. Doherty, *J. Environ. Forensic* 1 (2000) 83–93.
- [5] US EPA, Superfund <http://www.epa.gov/superfund>.
- [6] D. Mackay, W.-Y. Shiu, K.-C. Ma, S.C. Lee, *Handbook of Physical-chemical Properties and Environmental Fate for Organic Chemicals*, CRC Press, 2006.
- [7] A.M. Fan, *Reviews of Environmental Contamination and Toxicology*, Springer, 1988, pp. 55–92.
- [8] J.R. Boulding, EPA, *Environmental Engineering Sourcebook*, CRC Press, 1996, pp. 87–100.
- [9] L. Huang, Z. Yang, B. Li, J. Hu, W. Zhang, W.-C. Ying, *AIChE J.* 57 (2011) 542–550.
- [10] E. Moccia, A. Intiso, A. Ciatelli, A. Proto, F. Guarino, P. Iannece, S. Castiglione, F. Rossi, Use of *Zea mays* L. in phytoremediation of trichloroethylene, *Environ. Sci. Pollut. Res.* (2016), <http://dx.doi.org/10.1007/s11356-016-7570-8>, in press.
- [11] J. Costanza, J. Mulholland, K. Pennell, Kurt, *Effects of Thermal Treatments on the Chemical Reactivity of Trichloroethylene*, US EPA, 2007.
- [12] M. Romero-Sáez, D. Divakar, A. Aranzabal, J.R. González-Velasco, J.A. González-Marcos, *Appl. Catal. B: Environ.* 180 (2016) 210–218.
- [13] N. Blanch-Raga, A.E. Palomares, J. Martínez-Triguero, S. Valencia, *Appl. Catal. B: Environ.* (2016) 90–97.
- [14] D. Divakar, M. Romero-Sáez, B. Pereda-Ayo, A. Aranzabal, J.A. González-Marcos, J.R. González-Velasco, *Catal. Today* 176 (2011) 357–360.
- [15] R. López-Fonseca, J.I. Gutiérrez-Ortiz, J.R. González-Velasco, *Appl. Catal. A: Gen.* 271 (2004) 39–46.
- [16] N. Blanch-Raga, A.E. Palomares, J. Martínez-Triguero, M. Puche, G. Fetter, P. Bosch, *Appl. Catal. B: Environ.* 160 (2014) 129–134.
- [17] A. Aranzabal, M. Romero-Sáez, U. Elizundia, J.R. González-Velasco, J.A. González-Marcos, *J. Catal.* 296 (2012) 165–174.
- [18] M.B. Gawande, V.D.B. Bonifácio, R. Luque, P.S. Branco, R.S. Varma, *ChemSusChem* 7 (2014) 24–44.
- [19] R. Cucciniello, A. Proto, F. Rossi, O. Motta, *Atmos. Environ.* 79 (2013) 666–671.
- [20] S. Yang, J.N. Kondo, K. Hayashi, M. Hirano, K. Domen, H. Hosono, *Chem. Mater.* 16 (2004) 104–110.
- [21] M. Ruzsak, S. Witkowski, Z. Sojka, *Res. Chem. Intermed.* 33 (2007) 689–703.
- [22] M. Kitano, Y. Inoue, Y. Yamazaki, F. Hayashi, S. Kanbara, S. Matsuishi, T. Yokohama, S. Kim, M. Hara, H. Hosono, *Nat. Chem.* 4 (2012) 934–940.
- [23] F. Hayashi, Y. Tomota, M. Kitano, Y. Toda, T. Yokoyama, H. Hosono, *J. Am. Chem. Soc.* 136 (2014) 11698–11706.
- [24] A. Proto, R. Cucciniello, A. Genga, C. Capacchione, *Catal. Commun.* 68 (2015) 41–45.
- [25] M. Lacerda, J.T.S. Irvine, F.P. Glasser, A.R. West, *Nature* 332 (1988) 525–526.
- [26] M. Ruzsak, M. Inger, S. Witkowski, M. Wilk, A. Kotarba, Z. Sojka, *Catal. Lett.* 126 (2008) 72–77.
- [27] C. Li, D. Hirabayashi, K. Suzuki, *Appl. Catal. B: Environ.* 88 (2009) 351–360.
- [28] C. Li, D. Hirabayashi, K. Suzuki, *Mater. Res. Bull.* 46 (2011) 1307–1310.
- [29] A. Proto, R. Cucciniello, F. Rossi, O. Motta, *Environ. Sci. Pollut. Res.* 21 (2013) 3182–3186.
- [30] M. Mendez, R. Ciuraru, S. Gosselin, S. Batut, N. Visez, D. Petitprez, *Atmos. Chem. Phys.* 13 (2013) 11661–11673.
- [31] M. Teusner, R.A. De Souza, H. Krause, S.G. Ebbinghaus, B. Belghoul, M. Martin, *J. Phys. Chem. C* 119 (2015) 9721–9727.
- [32] A. Schmidt, M. Lerch, J.-P. Eufinger, J. Janek, I. Tranca, M.M. Islam, T. Bredow, R. Dolle, H.D. Wiemöfer, H. Boysen, M. Hölzel, *Solid State Ion.* 254 (2014) 48–58.
- [33] J.-P. Eufinger, A. Schmidt, M. Lerch, J. Janek, *Phys. Chem. Chem. Phys.* 17 (2015) 6844–6857.
- [34] A. Aranzabal, B. Pereda-Ayo, M. Pilar González-Marcos, J.A. González-Marcos, R. López-Fonseca, J.R. González-Velasco, *Chem. Pap.* 68 (2014) 1169–1186.